2015 IEEE International Conference on Robotics and Automation (ICRA)
Washington State Convention Center
Seattle, Washington, May 26-30, 2015

Hierarchical Cooperative Control Framework of Multiple Quadrotor-Manipulator Systems

Hyunsoo Yang and Dongjun Lee

***Abstract*— We propose an hierarchical control framework for multiple cooperative quadrotor-manipulator systems, which allows us to endow the common grasped object with a user-specified desired behavior (e.g., trajectory tracking, compliant interaction, etc.). To achieve this, our control framework consists of the following hierarchical layers: 1) object desired behavior design; 2) optimal cooperative force distribution; and 3) individual quadrotor-manipulator control based on object stiffness model, which can also take into account different dynamics characteristics of the (slower/coarse) quadrotor-platform and the (faster/fine) manipulator. Simulations of object transport and compliant interaction with three quadrotor-manipulator systems are performed to illustrate the theory.**

I. Introduction

The quadrotor platform has attracted extensive attention from researchers in the academia and the industry alike, with many strong results proposed particularly for the motion control of the quadrotors [1]–[5]. Although many number of useful applications (e.g., aerial photography, surveillance, entertainment, etc.), this pure motion control of the quadrotor is restricted to "passive tasks" with no physical interaction with objects or external environments, and we believe that, to be truly a versatile robotic platform, it is necessary to endow this quadrotor platform with the ability of manipulation and/or physical interaction.

Some attempts have been made along this line, particularly utilizing simple interacting/manipulating mechanisms to circumvent the quadrotor's limited payload (typically few hundreds grams), e.g.,: 1) operation using a simple unactuated tool (e.g., screw-driver) attached on the quadrotor [6], [7]; 2) operation using a simple gripper attached on the quadrotor [8]; and 3) payload transport using cable attached to the quadrotor was proposed in [9]. Although promising in terms of its mechanical simplicity and light weight, such simple tool, gripper or cable, yet, can only provide limited manipulation capability due to the lack of their actuation.

Aiming for dexterous aerial manipulation, quadrotor-manipulator (QM) systems have been recently considered (e.g., [10]–[15]). See Fig. 1. One of the key challenges in deploying this QM system is that its dynamics is fairly complicated with large degree-of-freedom (DOF) and the nonlinear dynamic quadrotor-manipulator coupling, while the control design itself is also hindered by the under-actuation of the quadrotor platform. Perhaps, due to this difficulty, majority of the QM system control results either considered the quadrotor and the manipulator separately with their dynamic coupling considered as disturbance (e.g., [10], [11]); or simplified the QM system to be fully-actuated kinematic/dynamic systems while not explicitly taking into account the quadrotor's under-actuation into their control design (e.g., [12], [15]). To address this dynamic complexity, in [16], we revealed that, albeit seemingly complicated, the QM system dynamics is in fact composed of the *completely-decoupled* centroid translation dynamics and the internal (or shape) dynamics (of the quadrotor's rotation and the manipulator's joint angles), with the former assuming the form of the standard under-actuated quadrotor dynamics and the latter the form of the standard fully-actuated robot dynamics (with no gravity). Exploiting this decomposition, in [16], we could also design a backstepping end-effector tracking control in a fairly straightforward fashion.

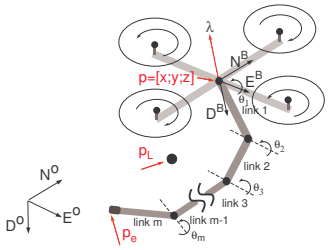

Fig. 1. QM system with m-DOF arm: $p = [x; y; z]$ is quadrotor platform's center position, $p_e = [x_e; y_e; z_e]$ the end-effector position, λ the thrust force input and p_{L} is the center-of-mass position of the total QM-system.

This QM system, yet, if deployed alone, would still suffer from the problem of limited payload (e.g., for AscTec® Pelican with 500g manipulator, remaining payload would be only around 100g). Multiple cooperative QM systems would then resolve this payload problem while also providing redundancy and manipulability unattainable by a single QM system. Results on these multiple cooperative QM systems, however, are very rare, perhaps due to the aforementioned dynamics complexity of even a single QM system. In fact, to our knowledge, all the results on aerial cooperative manipulation have been restricted to the quadrotors equipped only with simple tool, gripper or cable with some of them even assuming the quadrotors to be quasi-static (e.g., [17], [18], [19] , [20]).

In this paper, standing upon our recent result on the

Research supported in part by the Global Frontier R&D Program on Human-centered Interaction for Coexistence(NRF-2013M3A6A3079227), the Basic Science Research Program (2012-R1A2A2A0-1015797), and the Brain Korea 21 Plus Project in 2014(F14SN02D1310) of the National Research Foundation (NRF) of Korea funded by the Ministry of Education, Science & Technology (MEST).

The authors are with the Department of Mechanical & Aerospace Engineering, Seoul National University, Seoul, 151-744, Republic of Korea. E-mail: {yangssoo,djlee}@snu.ac.kr.

dynamics and control of the single QM system [16], we propose a novel hierarchical cooperative control framework for multiple dynamic QM systems, which can endow the cooperatively-grasped object with an user-specific target behavior according to various task objective. Our proposed control framework is hierarchical and also modular with the following layers/sub-modules (see Fig. 2):

- **Object behavior design**, which computes the required wrench for the cooperatively-grasped object to achieve the user-specific target behavior according to task objectives (e.g., trajectory tracking, velocity-field following, compliant interaction, etc.);
- **Optimal cooperative force distribution**, which optimally assign contact force of each QM system to cooperatively achieve the desired object behavior, while minimizing a certain cost function and respecting the friction-cone constraints to prevent slippage; and
- **Individual QM system control**, which extends the end-effector position control of [16] for the admittance-type contact force control of each QM system with unknown object stiffness model and force sensor/estimator [21], while also explicitly taking into account the different dynamics characteristics of the (slower/coarse) quadrotor and the (faster/fine) manipulator.

The rest of the paper is organized as follows. System modeling of a single QM system is presented in Sec. II, with a brief summary of the dynamics decomposition and end-effect position control in [16]. Our proposed hierarchical control framework and its constituting layers are presented in Sec. III with relevant simulation results. Sec. IV then concludes the paper.

II. Preliminary

A. Dynamics Modeling of QM System

In this paper, we deal with the cooperation of N QM systems, each with multi-DOF serial-link manipulator. See Fig. 1. The configuration of a single QM system can then be given by

$$q := [p; \phi; \theta] \in \Re^n, \quad n := 6 + m$$

where $p = [x; y; z] \in \Re^3$ is the quadrotor platform's center-of mass in the inertial NED-frame, $\phi = [\phi_r; \phi_p; \phi_y] \in \Re^3$ is the roll/pitch/yaw angles of the quadrotor, and $\theta = [\theta_1; \cdots; \theta_m] \in \Re^m$ is the joint angles of the manipulator.

The QM-system is under-actuated, that is, the control action for the QM-system is given by

$$\tau = [-\lambda R e_3; \tau_{\phi_r}; \tau_{\phi_p}; \tau_{\phi_y}; \tau_1; ...; \tau_m] \in \Re^n \qquad (1)$$

where $\lambda \in \Re$ is the thrust force, $R(\phi_r, \phi_p, \phi_y) \in$ SO(3) is the rotation matrix of the quadrotor parameterized by (ϕ_r, ϕ_p, ϕ_y), $e_3 = [0; 0; 1]$ is a basis vector representing the D-direction, and $(\tau_{\phi_r}, \tau_{\phi_p}, \tau_{\phi_y})$ and $\tau_i \in \Re$ are respectively the quadrotor's roll/pitch/yaw torques and that of each manipulator joints. $r = [\phi; \theta] \in \Re^{3+m}$ is fully-actuated with the torque input $(\tau_{\phi_r}, \tau_{\phi_p}, \tau_{\phi_y})$ and τ_i, while $p = [x; y; z] \in \Re^3$ is under-actuated with only the thrust force input λ, whose direction is fixed to the quadrotor body-fixed D-direction.

From the kinetic energy $\kappa = \frac{1}{2}\dot{q}^T M(r)\dot{q}$, where $M(r) \in \Re^{n\times n}$ is inertia matrix, and the gravitational potential energy $\varphi(q)$, Lagrange dynamics of the QM-system is given by

$$M(r)\ddot{q} + C(r, \dot{r})\dot{q} + g(r) = \tau + f \qquad (2)$$

where $C(r, \dot{r}) \in \Re^{n\times n}$ is the Coriolis matrix with $\dot{M} - 2C$ being skew-symmetric, $g(q) = \partial\varphi(q)/\partial q \in \Re^n$ is the gravitational force, $\tau \in \Re^n$ is the control action (1), and $f \in \Re^n$ is the external disturbance. Note that inertia matrix $M(r)$ is only a function of r due to symmetry in $E(3)$, thus dynamics is symmetric w.r.t. p if no gravity is present.

B. Dynamics Decomposition and Control of QM System

In [16], we showed that the QM system dynamics (2) is in fact composed of the following two decoupled dynamics:

$$m_L\ddot{p}_L + g_L = \tau_L + f_L \qquad (3)$$

$$M_E(r)\ddot{r} + C_E(r, \dot{r})\dot{r} = \tau_E + f_E \qquad (4)$$

where $p_L \in \Re^3$ is the center-of-mass position of the total QM system with $m_L > 0$ being its mass; $r = [\phi; \theta]$ is the internal rotation with $M_E(r),\ C_E(r, \dot{r}) \in \Re^{(3+m)\times(3+m)}$ being its inertia and Coriolis matrices respectively with skew-symmetric $\dot{M}_E - 2C_E$; $g_L \in \Re^3$ is the gravity vector, $\tau_L = -\lambda R e_3 \in \Re^3$ and $\tau_E \in \Re^{3+m}$ are the (under-actuated) thrust input for p_L and the fully-actuated control for r; and $f_L \in \Re^3$, $f_E \in \Re^{3+m}$ are transformed external disturbances.

This dynamics decomposition (3)-(4) possesses the following remarkable properties: 1) the two dynamics are completely decoupled from each other with no inertial, Coriolis and gravity couplings; 2) the center-of-mass p_L dynamics (3) has the form of the standard under-actuated quadrotor dynamics with $\tau_L = -\lambda R e_3$; 3) the internal rotation dynamics (4) has the form of the standard fully-actuated manipulator dynamics; and 4) gravity effect shows up only in (3) and not in (4). This decomposition structure (3)-(4) turns out to hold for general vehicle-manipulator systems (e.g., underwater ROV with arm, space robot equipped with manipulator, etc.). This decomposition (3)-(4) also generalizes the concept of virtual manipulator in [22] to the case with the gravity.

In [16], exploiting the dynamics decomposition (3)-(4). we proposed a trajectory tracking control for the QM system's end-effector position $p_e \in \Re^3$, which can be written as

$$\dot{p}_e = \dot{p}_L + B(r)\dot{r} \qquad (5)$$

where p_L and r are respectively the QM system center-of-mass position and the internal rotation, whose dynamics are decoupled in (3)-(4), and $B(r) \in \Re^{3\times(m+3)}$ is a Jacobian-like matrix from $\dot{r}$ to $\dot{p}_e$ with the inertial parameters embedded in it. Then, differentiating (5) and individually incorporating (3)-(4), in [16], we could design the control generation equation to achieve $p_e \to p_e^d$ s.t.,

$$\tau_L + m_L B M_E^{-1}[\tau_E - C_E\dot{r}] = -\gamma e_p - \alpha e_L + g_L + m_L[\ddot{p}_e^d - k\dot{e}_p - \frac{dB}{dt}\dot{r}] \qquad (6)$$

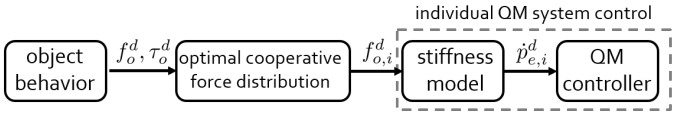

Fig. 2. Hierarchical cooperative control framework of multiple QM systems

where $\gamma, \alpha, k > 0$ are control gains, $e_p := p_e^d - p_e$, and $e_L := \dot{p}_L^d - \dot{p}_L$ with $\dot{p}_L^d := \dot{p}_e^d + k(p_e^d - p_e) - B(r)\dot{r}$. Satisfying this control equation (6) then guarantees that $(e_p, e_L) \to 0$ exponentially [16].

In the control generation equation (6), $\tau_L = -\lambda R e_3$ cannot be arbitrarily assigned due to the under-actuation. However, $\tau_E \in \Re^{m+3}$ is fully-actuated, thus, similar to the case of redundancy resolution, can be utilized to satisfy (6) even with the under-actuated τ_L. Exploiting this redundancy, in [16], we suggest to allocate the control to τ_L and τ_E s.t.,

$$\tau_L^d = -\gamma e_p - \alpha e_L + g_L + m_L[\ddot{p}_e^d - k\dot{e}_p - \tfrac{dB}{dt}\dot{r} - \zeta(r)] \quad (7)$$

$$m_L B M_E^{-1}[\tau_E - C_E \dot{r}] \quad (8)$$
$$= -\gamma e_p - \alpha e_L + g_L + m_L[\ddot{p}_e^d - k\dot{e}_p - \tfrac{dB}{dt}\dot{r}] - \tau_L$$

where, in (7), τ_L^d is the desired thrust input, whereas, in (8), τ_E is set to satisfy the control equation (6) even if $\tau_L \neq \tau_L^d$ due to the under-actuation, while τ_E in the nullspace of BM_E^{-1} is utilized to align the quadrotor orientation to that of τ_L^d. Also, in steady-state with $\tau_L \to \tau_L^d$, we have, from (7)-(8), $m_L B(r)\ddot{r} \to \zeta(r)$, which can encode a certian sub-task (e.g., singularity avoidance, etc.). This control allocation (7)-(8) then allows us to achieve the end-effector trajectory tracking $p_e \to p_e^d$ even in the presence of under-actuation with $\tau_L \to \tau_L^d$ and the steady-state sub-task $\zeta(t)$.

For our hierarchical cooperative control framework, in Sec. III, we will extend this position control (6) to enable each QM system to exert their desired contact force by using (uncertain) object stiffness model and force sensing/estimator, while also explicitly incorporating slower/coarse quadrotor dynamics and faster/fine manipulator dynamics.

III. Hierarchical Control Framework for Multiple QM Systems

For the cooperative control of multiple QM systems, here, we adopt an hierarchical and modular approach, where an hierarchy is constructed from the highest-level task (i.e., object behavior design such as object transport or compliant interaction between the grasped object and external environment) to the middle-level task (i.e., optimal distribution of the resultant object wrench for generating the target object behavior to each QM system's end-effector) and to the lowest-level task (i.e., individual QM system admittance-type end-effector force control to realize the optimally-assigned contact force), while also each layer can be modified/replaced according to task objectives. See Fig. 2. In the following, we will discuss each component of this hierarchical cooperative control framework in details.

A. Object Behavior Design

As stated above, depending on the task objective, the cooperatively-grasped object should exhibit a certain desired behavior such as trajectory tracking, compliant interaction, etc. The goal of the object behavior design block of our proposed control framework is to determine the object wrench to achieve the designated target behavior of the object. For this, we assume that the grasped object is a 6-DOF rigid-body, whose dynamics is given by:

$$m_o \ddot{p}_o + m_o g = f_o + f_{ext}$$
$$I\dot{w}_o + w_o \times I_o w_o = \tau_o + \tau_{ext}$$

where $m_o \in \Re$, $I_o \in \Re^{3\times3}$ are the mass and moment of inertia of the object, $p_o, w_o \in \Re^3$ are its position and angular velocity, $f_o, \tau_o \in \Re^3$ are the resultant force and torque exerted by the N QM systems' end-effectors, and $f_{ext}, \tau_{ext} \in \Re^3$ are its interaction force/torque with external environments.

We can then design f_o and τ_o to achieve some desired behavior of the grasped object. For instance, impedance interaction at the object center-of-mass with scaled apparent inertia with rotational spring behavior can be achieved by

$$f_o = \alpha f_{ext} + m_o g + m_o \ddot{p}_o^d + D(\dot{p}_o^d - \dot{p}_o) + K(p_o^d - p_o)$$
$$\tau_o = -\gamma w_o - \sigma[R_d^T R_o - R_o^T R_d]^\vee$$

where α is to scaling the apparant mass of the object at its center-of-mass, f_{ext} is external force which may be obtained by force sensor or disturbance observer [21], $p_o^d \in \Re^3$ is the desired object trajectory, $D, K \in \Re^{3\times3}$ are the symmetric and positive-definite damping and spring gains, R_d is the set-rotation for the rotational spring, γ, σ are the damping and the rotation stabilization gain for rotation dynamics and $[\cdot]^\vee$ denotes the operation $so(3) \to \Re^3$ [23]. This impedance type behavior can be used for physical interaction tasks with external environment, humans or another objects by changing its parameter to behave lighter/softer (i.e., low impedance) or heavier/stiffer (e.g., high impedance) than the original system. Note that, for such physical interaction tasks, we typically have small $(\ddot{p}_o, \dot{p}_o, w_o)$. Also note that with $\alpha = 0$ or $(f_{ext}, \tau_{ext}) \approx 0$, which typically true for the transport operation, the object transport can be achieved.

B. Optimal Cooperative Force Distribution

To realize the desired object wrench, $F_o := [f_o; \tau_o] \in \Re^6$, as designed in Sec. III-A, we then need to determine the contact force $f_{o,i}^d \in \Re^3$ exerted by each QM system's end-effector on the grasped object. For this, we utilize the following Jacobian relation between the object wrench F_o and the end-effector force $f_{o,i}$ s.t.,

$$F_o = J_o \bar{f}_o \quad (9)$$

where $J_o \in \Re^{6\times3N}$ is the object Jacobian and $\bar{f}_o = [f_{o,1}; \cdots, f_{o,N}] \in \Re^{3N}$ is the collection of the end-effector contact forces of all the QM systems, with $f_{o,i} \in \Re^3$ being the end-effector contact force of the i-th QM system, which contains both the normal and shear/friction forces as shown in Fig. 3. Here, we assumed that the contact between each QM system and the object is the point contact with friction and without moment transmission. The case of more general

contact scenarios will be studied in a future publication. Then, the end-effector force $f_{o,i}$ can be decomposed with respect to the object surface s.t.,

$$f_{o,i} = f_{n,i} \cdot u_{n,i} + f_{s1,i} \cdot u_{s1,i} + f_{s2,i} \cdot u_{s2,i}$$

where $u_{n,i}, u_{s1,i}, u_{s2,i} \in \Re^3$ are the normal and tangential directional unit vectors, which are orthogonal with each other; and $f_{n,i}, f_{s1,i}, f_{s2,i} \in \Re$ are the magnitude along each direction. See Fig. 3.

Here, in (9), $J_o \in \Re^{6\times 3N}$ is typically a fat matrix ($3N > 6$). Therefore, the solution of $\bar{f}_o$ of (9) is not unique with different "internal/null-space forces". Moreover, the contact force of each QM system should satisfy the friction cone constraint [24] to maintain the contact while avoiding slippage. We now formulate this problem of finding $\bar{f}_o$ as the following constrained optimization problem:

$$\begin{aligned} \min_{f_s, f_n} \quad & \alpha_1 f_s^T f_s + \alpha_2 f_n^T f_n \\ \text{subject to} \quad & F_o = J_o \mathcal{N} f_n + J_o \mathcal{T} f_s \\ & \sqrt{f_{s1,i}^2 + f_{s2,i}^2} \le \mu f_{n,i}, \ i = 1, 2, \cdots N \end{aligned} \tag{10}$$

where $\alpha_1, \alpha_2 > 0$ are the weights, $f_n := [f_{n,1}; \cdots; f_{n,N}] \in \Re^N$ and $f_s := [f_{s1,1}; f_{s2,1}; \cdots; f_{s1,N}; f_{s2,N}] \in \Re^{2N}$ are respectively the collections of the normal and shear friction force components of $f_{o,i}$ w.r.t. the object contact surface, $\mu > 0$ is the static friction coefficient, and $\mathcal{N} \in \Re^{3N\times N}$ and $\mathcal{T} \in \Re^{3N\times 2N}$ respectively identify the tangential and normal directions with their expressions given by

$$\mathcal{N} = \text{diag}(u_{n,1}, \cdots, u_{n,N}), \quad \mathcal{T} = \text{diag}(u_{s,1}, \cdots, u_{s,N}).$$

where $u_{s,i} = [u_{s1,i}, u_{s2,i}] \in \Re^{3\times 2}$ is the collection of the i-th QM system's tangential directional unit vectors.

For this constrained optimization problem, we choose $\alpha_1 > \alpha_2 > 0$ to ensure the shear/friction force $f_{s,i}$ to be low to have a better margin against the contact slippage, while also simultaneously preventing excessively large normal contact force. Note also that: 1) the equality constraint of (10) is merely a different representation of the object Jacobian relation (9), whereas the inequality constraint in (10) is to enforce the friction-cone condition to ensure no-slip contact. This optimization problem is convex and has the structure of force optimization problem (FOP), thus this can be formulated as a semidefinite programming problem (SDP) or a second-order cone problem (SOCP) [24], [25]. This FOP can be solved by standard numerical optimization method, however, to solve more faster depending on tasks, problem should be customized (e.g., dual problem [25]) rather than general SDP or SOCP. But, in this paper, for the case of three QM systems and not agile motion in III-D, standard method is sufficient to provide real-time solution.

Each individual QM system should then be able to exert this optimally-distributed contact force $f_{o,i}$. For this, we may attempt to devise a direct end-effector force control, which, yet, may not be straightforward to design here due to the presence of the quadrotor under-actuation along with the actuation redundancy of the QM system. Moreover, in practice, the robotic manipulator, which can be attached on the quadrotor platform, would likely have non-negligible joint friction. Even further, given the hardware and control precision limitations of currently available quadrotor platforms, the achievable speed of the cooperative manipulation of the grasped object would be rather slow. Due to this reason, in this paper, we adopt the admittance-type force control and, for that, in Sec. III-C, we will extend the position control law (6) to the case of uncertain object deformation model, while also explicitly taking into account the different dynamics characteristics of the quadrotor platform and the robotic manipulator.

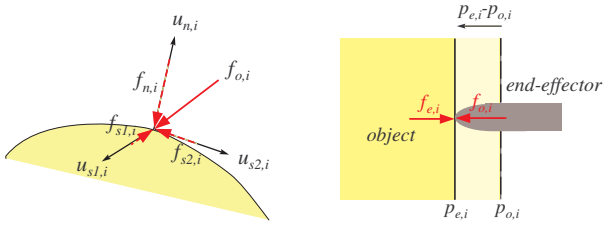

(a) Contact force decomposition (b) Object stiffness model

Fig. 3. Contact force decomposition and object stiffness model.

C. Force Control of QM System with Object Stiffness Model

To derive the admittance-type end-effector force control for each QM system, similar to [26], here, we assume that the deformation of the object is small so that it can be approximated by the linear stiffness model, i.e.,

$$f_{e,i} = -K_o(p_{e,i} - p_{o,i}) \tag{11}$$

where $f_{e,i} \in \Re^3$ is the contact force exerted by the object to the QM system's end-effector with $f_{e,i} = -f_{o,i}$, $p_{e,i}, p_{o,i} \in \Re^3$ are respectively the positions of the end-effector and the (undeformed) contact point of that end-effector on the grasped object, and $K_o \in \Re^{3\times 3}$ is the *uncertain* stiffness matrix. Here, we also assume that the deformation associated with each QM system's end-effector is independent from each other.

To achieve the admittance-type contact force control, we now design the evolution of the end-effector target position $p_{e,i}^d \in \Re^3$ s.t.,

$$\dot{p}_{e,i}^d := k_1(f_{e,i} - f_{e,i}^d) + k_2 \int (f_{e,i} - f_{e,i}^d)dt + \dot{p}_{o,i} \tag{12}$$

where $k_1, k_2 > 0$ are the PI control gains, $f_{e,i}$ is the contact force feedback, for which we assume force sensor or disturbance estimator for each QM system [21], and $f_{e,i}^d \in \Re^3$ is the desired contact force assigned by the optimal cooperative force distribution algorithm (10). Here, note that we can compute $p_{o,i}$ with the position and orientation sensing of the object center with the information on its undeformed shape.

Theorem 1 *Consider the N multiple cooperative QM systems with each of their dynamics given by* (3)-(4) *and their desired end-effector force given by $f_{e,i}^d$ (i.e., from* (10)*).*

Suppose that the object acceleration $\ddot{p}_o$ and the rate of change of each QM system's desired contact force $\dot{f}^d_{e,i}$ are bounded. Then, if we set the control τ_L, τ_E s.t.,

$$\tau_L + m_L B M_E^{-1}[\tau_E - C_E\dot{r}] = -f_L - m_L B M_E^{-1} f_E + g_L + m_L[\hat{\ddot{p}}^d_e - \beta\dot{e}_p - \gamma(e_f + \epsilon\int e_f dt) - \tfrac{dB}{dt}\dot{r}] \quad (13)$$

where $e_f := f_{e,i} - f^d_{e,i}$, $\hat{\ddot{p}}^d_{e,i} = \ddot{p}^d_{e,i} + \eta$ with bounded η, $\gamma, \beta, \epsilon > 0$ and $\epsilon < k_1 \cdot \lambda_{\min}[K_o]$, $(e_f, e_{fI}, \dot{e}_p)$ is ultimately bounded, where $e_{fI} := \int e_f dt + \dot{f}_d$ with $\dot{f}_d := (1/k_2)K_o^{-1}\dot{f}^d_{e,i}$ and $e_p := p_{e,i} - p^d_{e,i}$.

Proof: Using the object stiffness model (11) and the evolution equation (12), we have

$$\dot{e}_f = -K_o(\dot{p}^d_{e,i} - \dot{p}_{o,i}) - K_o\dot{e}_p - \dot{f}^d_{e,i} = -k_1 K_o e_f - k_2 K_o\int e_f dt - K_o\dot{e}_p - \dot{f}^d_{e,i} \quad (14)$$

From this, let us define the following Lyapunov function candidate:

$$V_1 := \frac{1}{2}e_f^T e_f + \frac{1}{2}e_{fI}^T k_2 K_o e_{fI} + \epsilon e_f^T e_{fI}$$

where ϵ is a small constant to make V_1 to be positive-definite and to be determined below. Then, using (12)-(14), the time derivative of V_1 is given by

$$\frac{dV_1}{dt} = -\begin{pmatrix} e_f \\ e_{fI}\end{pmatrix}^T \underbrace{\begin{bmatrix} k_1K_o - \epsilon I_3 & \frac{1}{2}\epsilon k_1 K_o \\ \frac{1}{2}\epsilon k_1 K_o & \epsilon k_2 K_o\end{bmatrix}}_{:=Q}\begin{pmatrix} e_f \\ e_{fI}\end{pmatrix} + \begin{bmatrix}\epsilon\ddot{f}_d & k_2 K_o \ddot{f}_d\end{bmatrix}\begin{pmatrix} e_f \\ e_{fI}\end{pmatrix} - \dot{e}_p^T K_o(e_f + \epsilon e_{fI}) \quad (15)$$

where $Q > 0$ for small enough $\epsilon < k_1 \cdot \lambda_{\min}[K_o]$. To proceed more, again, we define Lyapunov candidate function V_2:

$$V_2 := V_1 + \frac{1}{2\gamma}\dot{e}_p K_o \dot{e}_p$$

Time derivative is derived using (3), (4),

$$\frac{dV_2}{dt} = -\begin{pmatrix} e_f \\ e_{fI}\end{pmatrix}^T Q\begin{pmatrix} e_f \\ e_{fI}\end{pmatrix} + \begin{bmatrix}\epsilon\ddot{f}_d & k_2 K_o \ddot{f}_d\end{bmatrix}\begin{pmatrix} e_f \\ e_{fI}\end{pmatrix} - \frac{1}{\gamma}\dot{e}_p^T K_o[\gamma(e_f + \epsilon e_{fI}) - \ddot{e}_p] \quad (16)$$

where $\ddot{e}_p = \ddot{p}_{e,i}(\tau_L, \tau_E) - \ddot{p}^d_{e,i}(\dot{f}_{e,i}, \dot{f}^d_{e,i}, f_{e,i,}, f^d_{e,i}, \ddot{p}_{o,i})$. The first term is extended by dynamics (3)-(4) and (5) where

$$\ddot{p}_{e,i} = \frac{1}{m_L}[\tau_L + f_L - g_L] + B M_E^{-1}[\tau_E + f_E - C_E] + \dot{B}\dot{r}. \quad (17)$$

In the second term of $\ddot{e}_p$, $\ddot{p}^d_{e,i}$ is given by parameters in the parenthesis. $f_{e,i}$ is known from force sensor/estimator, $\dot{f}^d_{e,i}$, $\ddot{p}_{o,i}$ assumed to be bounded by assumption and $f^d_{e,i}$ is known from optimal cooperative force distribution. Then, all the parameters in the parenthesis are known or bounded, thus, we can write $\ddot{p}^d_{e,i} = \hat{\ddot{p}}^d_{e,i} - \eta$ where $\hat{\ddot{p}}^d_{e,i}$ is estimated from known parameter or numerically calculated and η is bounded remained term. From this, control generation equation (13) can be equivalently represented as following equation using (3)-(4) and (17)

$$\ddot{p}_{e,i} - \hat{\ddot{p}}^d_{e,i} = \gamma(e_f + \epsilon e_{fI} - \frac{1}{k_2}K_o^{-1}\dot{f}^d_{e,i}) - \beta\dot{e}_p. \quad (18)$$

Using this relation, time derivative $\dot{V}_2$ becomes

$$\frac{dV_2}{dt} = -\begin{pmatrix} e_f \\ e_{fI}\end{pmatrix}^T Q\begin{pmatrix} e_f \\ e_{fI}\end{pmatrix} - \frac{\beta}{\gamma}\dot{e}_p^T K_o \dot{e}_p + \begin{bmatrix}\epsilon\ddot{f}_d & K_o k_2 \ddot{f}_d\end{bmatrix}\begin{pmatrix} e_f \\ e_{fI}\end{pmatrix} + \frac{1}{\gamma}\dot{e}_p^T K_o \bar{\eta} \quad (19)$$

where $\bar{\eta} = \eta - \frac{1}{k_2}K_o^{-1}\dot{f}^d_{e,i}$ which is bounded. Then, all the terms, which are not negative definite, are bounded, thus are $(e_f, e_{fI}, \dot{e}_p)$ are ultimately bounded by control (13). ■

Note from Th. 1 that we can guarantee the desired force tracking by enforcing (13), even if the object stiffness K_o is unknown. Note also that, in the control input (13) with the target position dynamics (12), there is no usage of the object stiffness K_o. This proposed admittance-type force control (13) shares the similar development idea with the position tracking control of [16] (i.e., (7)-(8)). Yet it has been extended from (7)-(8) by incorporating the (unknown) object stiffness model K_o, the target position evolution equation, and the cross-coupling term (i.e., ϵ) to guarantee ultimately boundedness even in the presence of (inaccessible) $\dot{f}^d_{e,i}$, $\ddot{f}^d_{e,i}$.

We further modify this admittance-type force control here to explicitly into account the different dynamics characteristics of the (slower/coarse) quadrotor platform and the (faster/fine) robotic manipulator. More precisely, we assign the desired control generation equation (13) into the (under-actuated) quadrotor thrust control $\tau_L = -\lambda R e_3$ and the (fully-actuated) internal rotation dynamics control τ_E s.t.,

$$\tau^d_L = g_L + m_L[\mathrm{LPF}_{w_c(\sigma)}[\hat{\ddot{p}}^d_e] - \beta\dot{e}_p - \zeta(r)] - f_L \quad (20)$$

$$m_L B M_E^{-1}[\tau_E - C_E\dot{r}] = -f_L - m_L B M_E^{-1} f_E - \tau_L + g_L + m_L[\hat{\ddot{p}}^d_e - \beta\dot{e}_p - \gamma(e_f + \epsilon\int e_f dt) - \frac{dB}{dt}\dot{r}] \quad (21)$$

where LPF is a low pass filter operator and $w_c(\sigma)$ is the cut-off frequency of this LPF, which we define to be a function of the manipulability σ of the robot manipulator [27]. Also, similar to (7), here, we design the desired thrust input τ^d_L via (20), which will be achieved by using the internal rotation control τ_E in the null-space of BM_E^{-1}, whereas the other components of τ_E can still guarantee the control generation equation (13) even if $\tau_L \neq \tau^d_L$ via (20)

Here, additional terms are introduced by external force f_L, f_E from interaction with the grasped object. We design the control input τ_L and τ_E (20)-(21) to cancel out these external forces f_L, f_E. Physically, f_L affect the dynamics of the total QM system's center-of-mass position, so that thrust τ_L should resist f_L. On the other hand, f_E perturbs the quadrotor rotation and the manipulator configuration, thus, τ_E is used to cancel out f_E to maintain its posture.

Our proposed force control should also allow each QM systems to maintain its non-singular posture. For instance,

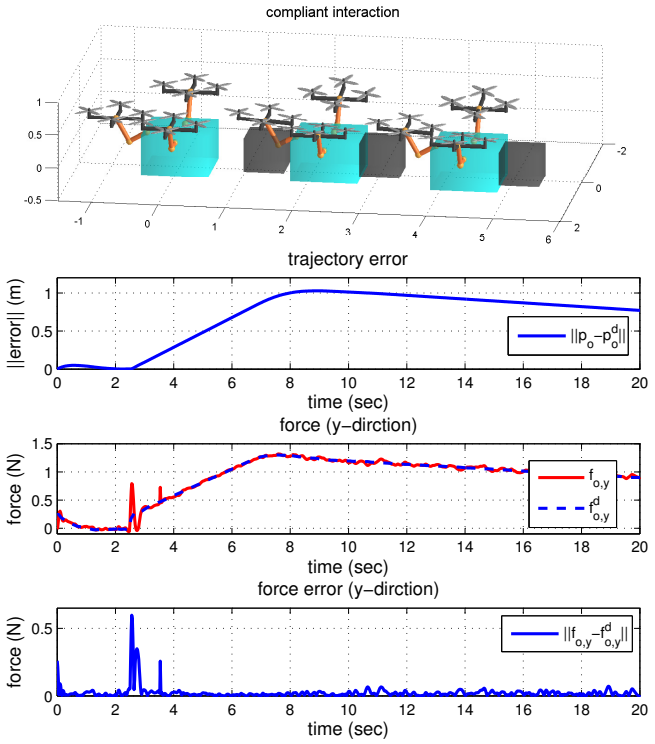

Fig. 4. Snapshots of the object pushing task using the multiple QM system under admittance-type force control with force profile.

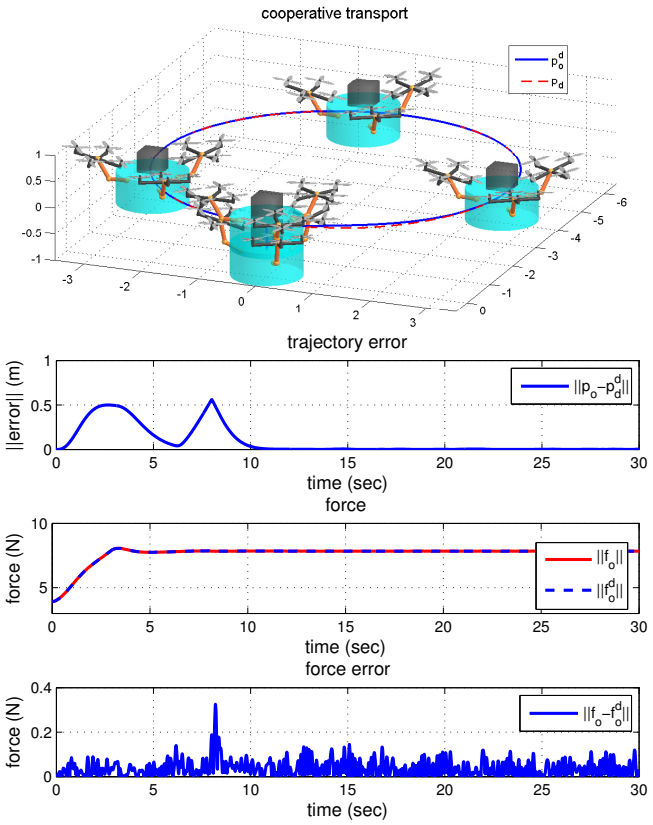

Fig. 5. Snapshots of the object transport using cooperative QM systmes control of compliant behavior with unknown mass and parameter adaptation.

when the QM system manipulates, the quadrotor platform should to keep a certain distance from the object for safety and the manipulator needs to recede from singular configuration which can cause instability. For this, the subtask $\zeta(r)$ utilized.

In (20), the low pass filter (LPF) is only applied to $\ddot{p}_e^d$, because gravity should be maintained by thrust τ_L and other terms are cancelled out or converge to small bounded value by Th. 1. Then, the LPF in the control equation (20) assigns low frequency slow motion to quadrotor platform via τ_L, then, the remained trajectory, which is high frequency component after substituting low frequency component, would be assigned to manipulator via τ_E. But, some infeasible desired motion can be generated without kinematic consideration. Since the manipulability is an index for measuring singularity, we propose to adapt the cut-off frequency depending on the manipulability using following relation

$$w_c = w_{c,min}\left(\frac{\sigma_{max}}{\sigma}\right)$$

where $w_{c,min}$ is the minimum cut-off frequency, σ is manipulability, σ_{max} is maximum value of the manipulability. From this equation, more specifically, if this manipulability σ is sufficient (i.e., $\sigma \approx \sigma_{max}$), the cut-off frequency of the LPF is set to be lower and almost all the motion would be assigned to the robotic manipulator via τ_E. On the other hand, near the singularity $\sigma \approx 0$, the cut-off frequency will be set to be higher and almost all the motion would be assigned to the quadrotor platform via τ_L.

D. Simulation

We perform two simulations using our proposed cooperative control framework. Here, the inertial parameter of quadrotor are $m_0 = 2kg$ and $(I_{xx}, I_{yy}, I_{zz}) = (1.24, 1.24, 1.24)kg \cdot m^2$ which are similar with AscTec® Pelican. 2-dof manipulator's inertial parameters are $(m_1, m_2) = (0.5, 0.4)kg$ and moment of inertia is assumed as cylinder and its length is $(l_1, l_2) = (0.4, 0.3)m$. Manipulator parameters are larger than real system to see dynamics effect. Moment of inertia is usually inaccurate, even though we can measure exact mass and length of the manipulator, thus, we add 20% error in the moment of inertia. Mass and stiffness of the object in the simulation, Fig. 4-5, are $m_o = 0.4kg$, $k_o = 200N/m$ which have $\sim 2cm$ of deformation to resist its weight. And also, here, we assume a force sensor to measure the exerting force which usually have white noise. To simulate this noise, we add a noise $w \sim \mathcal{N}(0, 0.04)$ with $3\sigma = 0.6$. Low pass filter with time constant $T = 0.5$ is also applied to reduce sensor noise, therefore, the measured force have delay due to filter.

The first simulation in Fig. 4 shows compliant interaction using the grasped object. For this, compliant behavior of the object is designed for object behavior design layer based on III-A. Here, we control the grasped object position to y-axis. Then, to achieve this desired behavior, the optimization provides the desired force distribution $f_{e,i}^d$. Using control (20)-(21), each QM system is controlled to achieve the

desired forces $f_{e,i}^d$. Then, the grasped object pushes the object in a stationary manner. At 2.5 second, the grasped object contacts with the another, black, object. Therefore, some position error is induced by repulsive force and the compliant behavior still can follow the desired force f_o^d, though bounded force error exists. See the bottom of Fig. 4.

In the second simulation, Fig. 5, we add an unknown mass on the stationary grasped object and perform circular trajectory tracking. At first, due to the unknown mass, grasped object goes to downward and position error is increased. However, the QM systems still can maintain the object grasping, even though the unknown mass disturbs position. Using the parameter adaptation of the unknown mass about the object dynamics [28], position error converges to zero and follows the desired trajectory. Note that, the second peak at 8 sec is caused by initial condition error (velocity and acceleration) of trajectory tracking.

IV. Conclusion

In this paper, we propose the cooperative control framework for multiple QM systems which consist of following hierarchical structure: 1) object bahavior design; 2) optimal cooperative force distribution; and 3) individual QM system control. The proposed control framework can be adapted to variable tasks which need different behavior by changing a specific control block rather than redesign the whole controller. And also, different types of individual QM system controllers are also applicable to this control framework without variation of the hierarchical structure. We extend previous result about the QM system position controller (6) from decoupled dynamics structure to admittance-like force control (13). Moreover, we propose how to control the individual QM system, using the decoupled dynamics (3)-(4), depending on different dynamics characteristics of the (under-actuated/slower/coarse) quadrotor platform and the (fully-actuated/faster/fine) manipulator. Simulation results of cooperative object transport and compliant interaction are presented.

Some possible future works include: 1) verification of the theory with real multiple QM systems; 2) modifying the controller to cover outdoor flight with visual servoing, visual-inertial sensor fusion, and force sensing/estimation; and 3) extend control framework to teleoperation.

References

[1] R. Mahony and T. Hamel. Robust trajectory tracking for a scale model autonomous helicopter. *International Jounal of Robust and Nonlinear Control*, 14:1035–1059, 2004.

[2] M-D Hua, T. Hamel, P. Morin, and C. Samson. A control approach for thrust-propelled underactuated vehicles and its application to vtol drones. *IEEE Transactions on Automatic Control*, 54(8):1837–1853, 2009.

[3] O. Purwin and R. D'Andrea. Performing aggressive maneuvers using iterative learning control. In *Proc. IEEE Int'l Conference on Robotics and Automation*, pages 1731–1736, 2009.

[4] D. J. Lee. Distributed backstepping control of multiple thrust-propelled vehicles on balanced graph. *Automatica*, 48(11):2971–2977, 2013.

[5] C. Ha, Z. Zuo, F. B. Choi, and D. J. Lee. Passivity-based adaptive backstepping control of quadrotor-type uavs. *Robotics and Autonomous Systems*, 62(9):1305–1315, 2014.

[6] D. J. Lee and C. Ha. Mechanics and control of quadrotors for tool operation. In *Proc. ASME Dynamics Systems and Control Conference*, pages 177–184, 2012.

[7] H. N. Nyugen and D. J. Lee. Hybrid force/motion control and internal dynamics of quadrotors for tool operation. In *Proc. IEEE Int'l Conference on Robotics and Automation*, 2013, to apear.

[8] V. Ghadiok, J. Goldin, and W. Ren. Autonomous indoor aerial gripping using a quadrotor. In *Proc. IEEE Int'l Conference on Intelligent Robots and Systems*, pages 4645–4651, 2011.

[9] I. Palunko, R. Fierro, and P. Cruz. Trajectory generation for swing-free maneuver of a quadrotor with suspended payload: a dynamic programming approach. In *Proc. IEEE Int'l Conference on Robotics and Automation*, pages 2691–2697, 2012.

[10] A.E. Jimenez-Cano, J. Martin, G. HereDia, and R. Cano A. Ollero. Control of an aerial robot with multi-link arm for assembly tasks. In *Proc. IEEE Int'l Conference on Robotics and Automation*, pages 4901–4906, 2013.

[11] C. Korpela, M. Orsag, and P. Oh M. Pekala. Dynamic stability of a mobile manipulating unmanned aerial vehicle. In *Proc. IEEE Int'l Conference on Robotics and Automation*, pages 4907–4912, 2013.

[12] V. Lippiello and F. Ruggiero. Exploiting redundancy in cartesian impedance control of uavs equipped with a robotic arm. In *Proc. IEEE Int'l Conference on Intelligent Robots and Systems*, pages 3768–3773, 2012.

[13] X. Ding and Y. Yu. Motion planning and stabilization control of a multipropeller multifunction aerial robot. *IEEE/ASME Transactions on Mechatronics*, 18(2):645–656, 2013.

[14] K. Kondak, K. Krieger, A. Albu-Schaeffer, M. Schwarzbach, M. Laiacker, I. Maza, A. Rodriguez-Castano, and A. Ollero. Closed-loop behavior of an autonomous helicopter equipped with a rootic arm for aerial manipulation tasks. *International Jounal of Advanced Robotic Systems*, 10(145):1–9, 2013.

[15] S. Kim, S. Choi, and H. J. Kim. Aerial manipulation using a quadrotor with a two dof robotic arm. In *Proc. IEEE/RSJ Int'l Conference on Intelligent Robots and Systems*, pages 4990–4995, 2013.

[16] H. Yang and D. J. Lee. Dynamics and control of quadrotor with robotic manipulator. In *Proc. IEEE Int'l Conference on Robotics and Automation*, pages 5544–5549, 2014.

[17] G. Gioioso, A. Franchi, S. Savietti, S. Scheggi, and D. Prattichizzo. The flying hand: a formation of uavs for cooperative serial telemanipulation. In *Proc. IEEE Int'l Conference on Robotics and Automation*, pages 4335–4341, 2014.

[18] D. Mellinger, M. Shomin, N. Michael, and V. Kumar. Cooperative grasping and transport using multiple quadrotors. In *Proc. Int'l Symposium on Distributed Autonomous Robotic Systems*, 2010.

[19] N. Michael, J. Fink, and V. Kumar. Cooperative manipulation and transportation with aerial robots. *Autonomous Robots*, 30(11):73–86, 2011.

[20] K. Sreenath and V. Kumar. Dynamics, control and planning for cooperative manipulation of payloads suspended by cables from multiple quadrotor robots. In *Robotics: Science and Systems*, 2013.

[21] F. Ruggiero, J. Cacace, H. Sadeghian, and V. Lippiello. Impedance control of vtol uavs with a momentum based external generalized forces estimator. In *Proc. IEEE Int'l Conference on Robotics and Automation*, pages 2093–2099, 2014.

[22] Z. Vafa and S. Dubowsky. The kinematics and dynamics of space manipulators: the virtual manipulator approach. *The International Jounals of Robotics Research*, 9(4):3–21, 1990.

[23] A. Sarlette, R. Sepulchre, and N. E. Leonard. Autonomous rigid body attitude synchronization. *Automatica*, 45(2):572–577, 2009.

[24] M. Buss, H. Hashimoto, and J. B. Moore. Dextrous hand grasping force optimization. *IEEE Transactions on Robotics and Automation*, 12(3):406–418, 1996.

[25] B. Wegbreit S. P. Boyd. Fast computation of optimal contact forces. *IEEE Transactions on Robotics*, 23(6):1117–1132, 2007.

[26] D. Sun, X. Shi, and Y. Liu. Modeling and cooperation of two-arm robotic system manipulating a deformable object. In *Proc. IEEE/RSJ Int'l Conference on Robotics and Automation*, pages 2346–2351, 1996.

[27] T. Yoshikawa. Manipulability of robotic mechanisms. *The International Journal of Robotics Research*, 4(3):3–9, 1985.

[28] J. E. Slotine and W. Li. *Applied nonlinear control*. Prentice Hall, 1991.